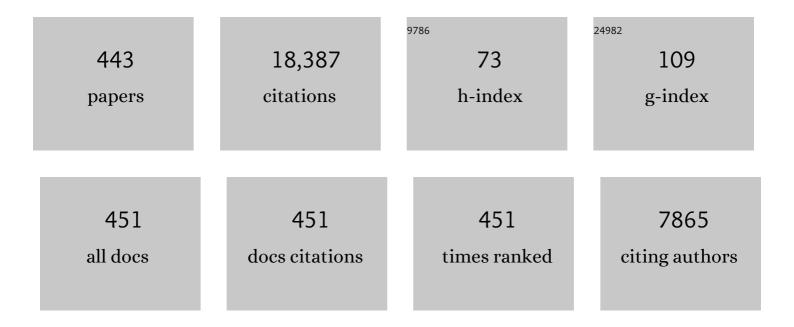
Derek Elsworth

List of Publications by Year in descending order

Source: https://exaly.com/author-pdf/4761444/publications.pdf Version: 2024-02-01



DEDEK FLOWODTH

#	Article	IF	CITATIONS
1	Seismicity triggered by fluid injection–induced aseismic slip. Science, 2015, 348, 1224-1226.	12.6	516
2	How sorption-induced matrix deformation affects gas flow in coal seams: A new FE model. International Journal of Rock Mechanics and Minings Sciences, 2008, 45, 1226-1236.	5.8	413
3	Interactions of multiple processes during CBM extraction: A critical review. International Journal of Coal Geology, 2011, 87, 175-189.	5.0	359
4	Changes in permeability caused by transient stresses: Field observations, experiments, and mechanisms. Reviews of Geophysics, 2012, 50, .	23.0	340
5	Permeability evolution in fractured coal: The roles of fracture geometry and water-content. International Journal of Coal Geology, 2011, 87, 13-25.	5.0	284
6	Failure of volcano slopes. Geotechnique, 1997, 47, 1-31.	4.0	259
7	Permeability evolution during progressive deformation of intact coal and implications for instability in underground coal seams. International Journal of Rock Mechanics and Minings Sciences, 2013, 58, 34-45.	5.8	201
8	Thermo-hydro-mechanical-chemical couplings controlling CH4 production and CO2 sequestration in enhanced coalbed methane recovery. Energy, 2019, 173, 1054-1077.	8.8	199
9	Dual poroelastic response of a coal seam to CO2 injection. International Journal of Greenhouse Gas Control, 2010, 4, 668-678.	4.6	193
10	Multiporosity/multipermeability approach to the simulation of naturally fractured reservoirs. Water Resources Research, 1993, 29, 1621-1633.	4.2	188
11	A model of coal–gas interaction under variable temperatures. International Journal of Coal Geology, 2011, 86, 213-221.	5.0	186
12	Thermal–hydrologic–mechanical–chemical processes in the evolution of engineered geothermal reservoirs. International Journal of Rock Mechanics and Minings Sciences, 2009, 46, 855-864.	5.8	185
13	Numerical simulation of thermal-hydrologic-mechanical-chemical processes in deformable, fractured porous media. International Journal of Rock Mechanics and Minings Sciences, 2009, 46, 842-854.	5.8	179
14	Permeability evolution in fractured coal — Combining triaxial confinement with X-ray computed tomography, acoustic emission and ultrasonic techniques. International Journal of Coal Geology, 2014, 122, 91-104.	5.0	178
15	Pore Structure Characterization of Coal by Synchrotron Small-Angle X-ray Scattering and Transmission Electron Microscopy. Energy & Fuels, 2014, 28, 3704-3711.	5.1	160
16	Evolution of coal permeability from stress-controlled to displacement-controlled swelling conditions. Fuel, 2011, 90, 2987-2997.	6.4	156
17	Evolution of permeability in a natural fracture: Significant role of pressure solution. Journal of Geophysical Research, 2004, 109, .	3.3	152
18	Evolution of fracture permeability through fluid–rock reaction under hydrothermal conditions. Earth and Planetary Science Letters, 2006, 244, 186-200.	4.4	148

#	Article	IF	CITATIONS
19	Shearâ€induced dilatancy of fluidâ€saturated faults: Experiment and theory. Journal of Geophysical Research, 2009, 114, .	3.3	148
20	Modelling and optimization of enhanced coalbed methane recovery using CO2/N2 mixtures. Fuel, 2019, 253, 1114-1129.	6.4	146
21	Effect of the effective stress coefficient and sorption-induced strain on the evolution of coal permeability: Experimental observations. International Journal of Greenhouse Gas Control, 2011, 5, 1284-1293.	4.6	143
22	Impact of transition from local swelling to macro swelling on the evolution of coal permeability. International Journal of Coal Geology, 2011, 88, 31-40.	5.0	143
23	Flowâ€Deformation Response of Dualâ€Porosity Media. Journal of Geotechcnical Engineering, 1992, 118, 107-124.	0.4	142
24	Understanding induced seismicity. Science, 2016, 354, 1380-1381.	12.6	139
25	Evaluation of stress-controlled coal swelling processes. International Journal of Coal Geology, 2010, 83, 446-455.	5.0	137
26	Linking gas-sorption induced changes in coal permeability to directional strains through a modulus reduction ratio. International Journal of Coal Geology, 2010, 83, 21-30.	5.0	136
27	Influence of the effective stress coefficient and sorption-induced strain on the evolution of coal permeability: Model development and analysis. International Journal of Greenhouse Gas Control, 2012, 8, 101-110.	4.6	136
28	Development of anisotropic permeability during coalbed methane production. Journal of Natural Gas Science and Engineering, 2010, 2, 197-210.	4.4	135
29	Permeability reduction of a natural fracture under net dissolution by hydrothermal fluids. Geophysical Research Letters, 2003, 30, .	4.0	134
30	A mechanistic model for compaction of granular aggregates moderated by pressure solution. Journal of Geophysical Research, 2003, 108, .	3.3	130
31	Dike intrusion as a trigger for large earthquakes and the failure of volcano flanks. Journal of Geophysical Research, 1995, 100, 6005-6024.	3.3	124
32	A dual poroelastic model for CO2-enhanced coalbed methane recovery. International Journal of Coal Geology, 2011, 86, 177-189.	5.0	124
33	Frictional stabilityâ€permeability relationships for fractures in shales. Journal of Geophysical Research: Solid Earth, 2017, 122, 1760-1776.	3.4	120
34	The effect of natural fractures on hydraulic fracturing propagation in coal seams. Journal of Petroleum Science and Engineering, 2017, 150, 180-190.	4.2	120
35	Breakdown pressure and fracture surface morphology of hydraulic fracturing in shale with H 2 O, CO 2 and N 2. Geomechanics and Geophysics for Geo-Energy and Geo-Resources, 2016, 2, 63-76.	2.9	119
36	Fault zone restrengthening and frictional healing: The role of pressure solution. Journal of Geophysical Research, 2005, 110, .	3.3	116

#	Article	IF	CITATIONS
37	Permeability evolution of fluid-infiltrated coal containing discrete fractures. International Journal of Coal Geology, 2011, 85, 202-211.	5.0	113
38	Effects of bedding on the dynamic indirect tensile strength of coal: Laboratory experiments and numerical simulation. International Journal of Coal Geology, 2014, 132, 81-93.	5.0	113
39	Experimental evaluation of CO 2 enhanced recovery of adsorbed-gas from shale. International Journal of Coal Geology, 2017, 179, 211-218.	5.0	112
40	Surface characteristics and permeability enhancement of shale fractures due to water and supercritical carbon dioxide fracturing. Journal of Petroleum Science and Engineering, 2018, 165, 284-297.	4.2	112
41	Analysis of coupled gas flow and deformation process with desorption and Klinkenberg effects in coal seams. International Journal of Rock Mechanics and Minings Sciences, 2007, 44, 971-980.	5.8	111
42	The Influence of Fracturing Fluids on Fracturing Processes: A Comparison Between Water, Oil and SC-CO2. Rock Mechanics and Rock Engineering, 2018, 51, 299-313.	5.4	110
43	Flank collapse triggered by intrusion: the Canarian and Cape Verde Archipelagoes. Journal of Volcanology and Geothermal Research, 1999, 94, 323-340.	2.1	106
44	Spontaneous switching of permeability changes in a limestone fracture with net dissolution. Water Resources Research, 2004, 40, .	4.2	106
45	A coupled flow-stress-damage model for groundwater outbursts from an underlying aquifer into mining excavations. International Journal of Rock Mechanics and Minings Sciences, 2007, 44, 87-97.	5.8	105
46	Experimental investigation on dynamic strength and energy dissipation characteristics of gas outburstâ€prone coal. Energy Science and Engineering, 2020, 8, 1015-1028.	4.0	100
47	Permeability Evolution in Natural Fractures Subject to Cyclic Loading and Gouge Formation. Rock Mechanics and Rock Engineering, 2016, 49, 3463-3479.	5.4	98
48	Laboratory evidence for particle mobilization as a mechanism for permeability enhancement via dynamic stressing. Earth and Planetary Science Letters, 2014, 392, 279-291.	4.4	97
49	Microcrack-based coupled damage and flow modeling of fracturing evolution in permeable brittle rocks. Computers and Geotechnics, 2013, 49, 226-244.	4.7	94
50	Impact of CO2 injection and differential deformation on CO2 injectivity under in-situ stress conditions. International Journal of Coal Geology, 2010, 81, 97-108.	5.0	93
51	A critical evaluation of unconventional gas recovery from the marcellus shale, northeastern United States. KSCE Journal of Civil Engineering, 2011, 15, 679-687.	1.9	93
52	Geomechanics of CO 2 enhanced shale gas recovery. Journal of Natural Gas Science and Engineering, 2015, 26, 1607-1619.	4.4	93
53	Modeling of subsidence and stress-dependent hydraulic conductivity for intact and fractured porous media. Rock Mechanics and Rock Engineering, 1994, 27, 209-234.	5.4	92
54	Linking stress-dependent effective porosity and hydraulic conductivity fields to RMR. International Journal of Rock Mechanics and Minings Sciences, 1999, 36, 581-596.	5.8	91

#	Article	IF	CITATIONS
55	Production optimization in fractured geothermal reservoirs by coupled discrete fracture network modeling. Geothermics, 2016, 62, 131-142.	3.4	90
56	Fabric induced weakness of tectonic faults. Geophysical Research Letters, 2010, 37, .	4.0	89
57	Implications of Magma Transfer Between Multiple Reservoirs on Eruption Cycling. Science, 2008, 322, 246-248.	12.6	87
58	Characterization of Coalbed Methane Reservoirs at Multiple Length Scales: A Cross-Section from Southeastern Ordos Basin, China. Energy & Fuels, 2014, 28, 5587-5595.	5.1	87
59	Instability and collapse of hazardous gas-pressurized lava domes. Geophysical Research Letters, 2000, 27, 1-4.	4.0	85
60	Unprecedented pressure increase in deep magma reservoir triggered by lava-dome collapse. Geophysical Research Letters, 2006, 33, .	4.0	84
61	Fracture spacing in layered materials: A new explanation based on two-dimensional failure process modeling. Numerische Mathematik, 2008, 308, 49-72.	1.4	84
62	Mechanical Behavior of Methane Infiltrated Coal: the Roles of Gas Desorption, Stress Level and Loading Rate. Rock Mechanics and Rock Engineering, 2013, 46, 945-958.	5.4	84
63	Why shale permeability changes under variable effective stresses: New insights. Fuel, 2018, 213, 55-71.	6.4	83
64	Complex evolution of coal permeability during CO2 injection under variable temperatures. International Journal of Greenhouse Gas Control, 2012, 9, 281-293.	4.6	82
65	Frictional strength and strain weakening in simulated fault gouge: Competition between geometrical weakening and chemical strengthening. Journal of Geophysical Research, 2010, 115, .	3.3	79
66	Microcrack-based geomechanical modeling of rock-gas interaction during supercritical CO2 fracturing. Journal of Petroleum Science and Engineering, 2018, 164, 91-102.	4.2	79
67	Analysis of thermally induced changes in fractured rock permeability during 8 years of heating and cooling at the Yucca Mountain Drift Scale Test. International Journal of Rock Mechanics and Minings Sciences, 2008, 45, 1373-1389.	5.8	78
68	In situ observations on the coupling between hydraulic diffusivity and displacements during fault reactivation in shales. Journal of Geophysical Research: Solid Earth, 2015, 120, 7729-7748.	3.4	78
69	CO ₂ /CH ₄ Competitive Adsorption in Shale: Implications for Enhancement in Gas Production and Reduction in Carbon Emissions. Environmental Science & Technology, 2019, 53, 9328-9336.	10.0	78
70	Role of proppant distribution on the evolution of hydraulic fracture conductivity. Journal of Petroleum Science and Engineering, 2018, 166, 249-262.	4.2	77
71	Coupled mechanical and chemical processes in engineered geothermal reservoirs with dynamic permeability. International Journal of Rock Mechanics and Minings Sciences, 2010, 47, 1339-1348.	5.8	76
72	Nanopore characterization of mine roof shales by SANS, nitrogen adsorption, and mercury intrusion: Impact on water adsorption/retention behavior. International Journal of Coal Geology, 2018, 200, 173-185.	5.0	75

#	Article	IF	CITATIONS
73	Compaction of a Rock Fracture Moderated by Competing Roles of Stress Corrosion and Pressure Solution. Pure and Applied Geophysics, 2008, 165, 1289-1306.	1.9	74
74	Healing of simulated fault gouges aided by pressure solution: Results from rock analogue experiments. Journal of Geophysical Research, 2008, 113, .	3.3	74
75	A continuum model for coupled stress and fluid flow in discrete fracture networks. Geomechanics and Geophysics for Geo-Energy and Geo-Resources, 2016, 2, 43-61.	2.9	74
76	Evolution of coal permeability: Contribution of heterogeneous swelling processes. International Journal of Coal Geology, 2011, 88, 152-162.	5.0	73
77	Analysis of fluid injectionâ€induced fault reactivation and seismic slip in geothermal reservoirs. Journal of Geophysical Research: Solid Earth, 2014, 119, 3340-3353.	3.4	73
78	A fully coupled multidomain and multiphysics model for evaluation of shale gas extraction. Fuel, 2020, 278, 118214.	6.4	73
79	Water Vapor Sorption Properties of Illinois Shales Under Dynamic Water Vapor Conditions: Experimentation and Modeling. Water Resources Research, 2019, 55, 7212-7228.	4.2	71
80	Coal permeability maps under the influence of multiple coupled processes. International Journal of Coal Geology, 2018, 187, 71-82.	5.0	70
81	Permeability evolution in sorbing media: analogies between organicâ€rich shale and coal. Geofluids, 2016, 16, 43-55.	0.7	69
82	Chemically and mechanically mediated influences on the transport and mechanical characteristics of rock fractures. International Journal of Rock Mechanics and Minings Sciences, 2009, 46, 80-89.	5.8	67
83	Optimizing enhanced coalbed methane recovery for unhindered production and CO2 injectivity. International Journal of Greenhouse Gas Control, 2012, 11, 86-97.	4.6	67
84	Estimation and modeling of coal pore accessibility using small angle neutron scattering. Fuel, 2015, 161, 323-332.	6.4	67
85	Reassessment of coal permeability evolution using steady-state flow methods: The role of flow regime transition. International Journal of Coal Geology, 2019, 211, 103210.	5.0	66
86	Scale effects and strength anisotropy in coal. International Journal of Coal Geology, 2018, 195, 37-46.	5.0	63
87	Characterization of rock fissure hydraulic conductivity using idealized wall roughness profiles. International Journal of Rock Mechanics and Mining Sciences, 1986, 23, 233-243.	0.0	61
88	Uniaxial strength and failure in sandstone containing a pre-existing 3-D surface flaw. International Journal of Fracture, 2015, 194, 59-79.	2.2	61
89	Laboratory investigations of gas flow behaviors in tight anthracite and evaluation of different pulse-decay methods on permeability estimation. International Journal of Coal Geology, 2015, 149, 118-128.	5.0	61
90	Numerical study of a stress dependent triple porosity model for shale gas reservoirs accommodating gas diffusion in kerogen. Journal of Natural Gas Science and Engineering, 2016, 32, 423-438.	4.4	59

#	Article	IF	CITATIONS
91	The role of gas desorption on gas outbursts in underground mining of coal. Geomechanics and Geophysics for Geo-Energy and Geo-Resources, 2016, 2, 151-171.	2.9	59
92	Effect of CO2 injection on heterogeneously permeable coalbed reservoirs. Fuel, 2014, 135, 509-521.	6.4	58
93	Re-evaluating adsorbed and free methane content in coal and its ad- and desorption processes analysis. Chemical Engineering Journal, 2022, 428, 131946.	12.7	58
94	Effects of local rock heterogeneities on the hydromechanics of fractured rocks using a digital-image-based technique. International Journal of Rock Mechanics and Minings Sciences, 2006, 43, 1182-1199.	5.8	57
95	Influence of shear and deviatoric stress on the evolution of permeability in fractured rock. Journal of Geophysical Research, 2009, 114, .	3.3	57
96	Failure mechanisms in coal: Dependence on strain rate and microstructure. Journal of Geophysical Research: Solid Earth, 2014, 119, 6924-6935.	3.4	56
97	Dual-damage constitutive model to define thermal damage in rock. International Journal of Rock Mechanics and Minings Sciences, 2020, 126, 104185.	5.8	56
98	A numerical model simulating reactive transport and evolution of fracture permeability. International Journal for Numerical and Analytical Methods in Geomechanics, 2006, 30, 1039-1062.	3.3	55
99	A mechanistic model for permeability evolution in fractured sorbing media. Journal of Geophysical Research, 2012, 117, .	3.3	55
100	Geological and hydrological controls on water coproduced with coalbed methane in Liulin, eastern Ordos basin, China. AAPG Bulletin, 2015, 99, 207-229.	1.5	54
101	The influence of Preslip Sealing on the Permeability Evolution of Fractures and Faults. Geophysical Research Letters, 2018, 45, 166-175.	4.0	54
102	Diagenetic sequences of continuously deposited tight sandstones in various environments: A case study from upper Paleozoic sandstones in the Linxing area, eastern Ordos basin, China. AAPG Bulletin, 2019, 103, 2757-2783.	1.5	54
103	An Experimental Study of Effect of High Temperature on the Permeability Evolution and Failure Response of Granite Under Triaxial Compression. Rock Mechanics and Rock Engineering, 2020, 53, 4403-4427.	5.4	54
104	Evaluation of volcano flank instability triggered by dyke intrusion. Geological Society Special Publication, 1996, 110, 45-53.	1.3	52
105	Three-dimensional effects of hydraulic conductivity enhancement and desaturation around mined panels. International Journal of Rock Mechanics and Minings Sciences, 1997, 34, 1139-1152.	5.8	52
106	Roles of coal heterogeneity on evolution of coal permeability under unconstrained boundary conditions. Journal of Natural Gas Science and Engineering, 2013, 15, 38-52.	4.4	52
107	Propagation, proppant transport and theÂevolution of transport properties of hydraulic fractures. Journal of Fluid Mechanics, 2018, 855, 503-534.	3.4	52
108	Mechanistic analysis of coal permeability evolution data under stress-controlled conditions. International Journal of Rock Mechanics and Minings Sciences, 2018, 110, 36-47.	5.8	52

#	Article	lF	CITATIONS
109	Experiment and modeling to evaluate the effects of proppant-pack diagenesis on fracture treatments. Journal of Petroleum Science and Engineering, 2010, 74, 67-76.	4.2	51
110	Permeability evolution of propped artificial fractures in coal on injection of CO2. Journal of Petroleum Science and Engineering, 2015, 133, 695-704.	4.2	51
111	The influence of thermal-hydraulic-mechanical- and chemical effects on the evolution of permeability, seismicity and heat production in geothermal reservoirs. Geothermics, 2015, 53, 385-395.	3.4	51
112	Evolution of permeability during the process of shale gas extraction. Journal of Natural Gas Science and Engineering, 2018, 49, 94-109.	4.4	51
113	Effect of coal maturity on CO2-based hydraulic fracturing process in coal seam gas reservoirs. Fuel, 2019, 236, 179-189.	6.4	51
114	Influence of gas adsorption induced non-uniform deformation on the evolution of coal permeability. International Journal of Rock Mechanics and Minings Sciences, 2019, 114, 71-78.	5.8	51
115	Modeling of naturally fractured reservoirs using deformation dependent flow mechanism. International Journal of Rock Mechanics and Mining Sciences, 1993, 30, 1185-1191.	0.0	50
116	A fully-coupled hydrological–mechanical–chemical model for fracture sealing and preferential opening. International Journal of Rock Mechanics and Minings Sciences, 2006, 43, 23-36.	5.8	50
117	Impact of Gas Adsorption Induced Coal Matrix Damage on the Evolution of Coal Permeability. Rock Mechanics and Rock Engineering, 2013, 46, 1353-1366.	5.4	50
118	An improved permeability evolution model and its application in fractured sorbing media. Journal of Natural Gas Science and Engineering, 2018, 56, 222-232.	4.4	50
119	Laboratory assessment of the equivalent apertures of a rock fracture. Geophysical Research Letters, 1993, 20, 1387-1390.	4.0	49
120	Breakdown pressures due to infiltration and exclusion in finite length boreholes. Journal of Petroleum Science and Engineering, 2015, 127, 329-337.	4.2	49
121	Permeability Evolution and Frictional Stability of Fabricated Fractures With Specified Roughness. Journal of Geophysical Research: Solid Earth, 2018, 123, 9355-9375.	3.4	48
122	Mineralogical Controls on Frictional Strength, Stability, and Shear Permeability Evolution of Fractures. Journal of Geophysical Research: Solid Earth, 2018, 123, 3549-3563.	3.4	47
123	Analysis of Stress-dependent Permeability in Nonorthogonal Flow and Deformation Fields. Rock Mechanics and Rock Engineering, 1999, 32, 195-219.	5.4	46
124	Frictionâ€5tabilityâ€Permeability Evolution of a Fracture in Granite. Water Resources Research, 2018, 54, 9901-9918.	4.2	46
125	Effect of temperature and confining pressure on the evolution of hydraulic and heat transfer properties of geothermal fracture in granite. Applied Energy, 2020, 272, 115290.	10.1	46
126	Thermal permeability enhancement of blocky rocks: One-dimensional flows. International Journal of Rock Mechanics and Mining Sciences, 1989, 26, 329-339.	0.0	45

#	Article	IF	CITATIONS
127	Evaluation of fully-coupled strata deformation and groundwater flow in response to longwall mining. International Journal of Rock Mechanics and Minings Sciences, 1997, 34, 1187-1199.	5.8	45
128	Numerical modelling of coupled flow and deformation in fractured rock specimens. International Journal for Numerical and Analytical Methods in Geomechanics, 1999, 23, 141-160.	3.3	45
129	Magmaâ€sponge hypothesis and stratovolcanoes: Case for a compressible reservoir and quasiâ€steady deep influx at SoufriA¨re Hills Volcano, Montserrat. Geophysical Research Letters, 2010, 37, .	4.0	45
130	Three stages of methane adsorption capacity affected by moisture content. Fuel, 2018, 231, 352-360.	6.4	45
131	Thermal-hydrologic mechanism for rainfall-triggered collapse of lava domes. Geology, 2004, 32, 969.	4.4	44
132	Permeability evolution during dynamic stressing of dual permeability media. Journal of Geophysical Research, 2012, 117, .	3.3	44
133	Linking permeability to crack density evolution in thermally stressed rocks under cyclic loading. Geophysical Research Letters, 2013, 40, 2590-2595.	4.0	43
134	Distinct element modeling of strength variation in jointed rock masses under uniaxial compression. Geomechanics and Geophysics for Geo-Energy and Geo-Resources, 2016, 2, 11-24.	2.9	43
135	Experimental simulation of the hydraulic fracture propagation in an anthracite coal reservoir in the southern Qinshui basin, China. Journal of Petroleum Science and Engineering, 2018, 168, 400-408.	4.2	43
136	A hybrid boundary element-finite element analysis procedure for fluid flow simulation in fractured rock masses. International Journal for Numerical and Analytical Methods in Geomechanics, 1986, 10, 569-584.	3.3	42
137	Flow rate dictates permeability enhancement during fluid pressure oscillations in laboratory experiments. Journal of Geophysical Research: Solid Earth, 2015, 120, 2037-2055.	3.4	42
138	Rapid decompression and desorption induced energetic failure in coal. Journal of Rock Mechanics and Geotechnical Engineering, 2015, 7, 345-350.	8.1	42
139	Fracture evolution in artificial bedded rocks containing a structural flaw under uniaxial compression. Engineering Geology, 2019, 250, 130-141.	6.3	42
140	Preliminary evaluation of gas content of the No. 2 coal seam in the Yanchuannan area, southeast Ordos basin, China. Journal of Petroleum Science and Engineering, 2014, 122, 675-689.	4.2	41
141	Hydraulic fracturing with leakoff in a pressure-sensitive dual porosity medium. International Journal of Rock Mechanics and Minings Sciences, 2018, 107, 55-68.	5.8	41
142	Controls of CO2–N2 gas flood ratios on enhanced shale gas recovery and ultimate CO2 sequestration. Journal of Petroleum Science and Engineering, 2019, 179, 1037-1045.	4.2	41
143	Effect of mineralogy on friction-dilation relationships for simulated faults: Implications for permeability evolution in caprock faults. Geoscience Frontiers, 2020, 11, 439-450.	8.4	41
144	Lithofacies and pore characterization of the Lower Permian Shanxi and Taiyuan shales in the southern North China Basin. Journal of Natural Gas Science and Engineering, 2016, 36, 644-661.	4.4	40

#	Article	IF	CITATIONS
145	A relation to predict the failure of materials and potential application to volcanic eruptions and landslides. Scientific Reports, 2016, 6, 27877.	3.3	39
146	A damage mechanics approach to the simulation of hydraulic fracturing/shearing around a geothermal injection well. Computers and Geotechnics, 2016, 71, 338-351.	4.7	39
147	Sedimentary characteristics of the Lower Cambrian Niutitang shale in the southeast margin of Sichuan Basin, China. Journal of Natural Gas Science and Engineering, 2016, 36, 1140-1150.	4.4	39
148	Effects of microstructure on water imbibition in sandstones using Xâ€ray computed tomography and neutron radiography. Journal of Geophysical Research: Solid Earth, 2017, 122, 4963-4981.	3.4	39
149	A model to evaluate the transient hydraulic response of threeâ€dimensional sparsely fractured rock masses. Water Resources Research, 1986, 22, 1809-1819.	4.2	37
150	Evaluation of groundwater flow into mined panels. International Journal of Rock Mechanics and Mining Sciences, 1993, 30, 71-79.	0.0	37
151	Vulcanian explosion at Soufrière Hills Volcano, Montserrat on March 2004 as revealed by strain data. Geophysical Research Letters, 2010, 37, .	4.0	37
152	Failure response of composite rock-coal samples. Geomechanics and Geophysics for Geo-Energy and Geo-Resources, 2018, 4, 175-192.	2.9	37
153	Some aspects of mining under aquifers in China. Mining Science and Technology, 1990, 10, 81-91.	0.0	36
154	Unique and remarkable dilatometer measurements of pyroclastic flow–generated tsunamis. Geology, 2007, 35, 25.	4.4	36
155	Significant effect of grain size distribution on compaction rates in granular aggregates. Earth and Planetary Science Letters, 2009, 284, 386-391.	4.4	36
156	A dual-scale approach to model time-dependent deformation, creep and fracturing of brittle rocks. Computers and Geotechnics, 2014, 60, 61-76.	4.7	36
157	Predicting timeâ€ŧoâ€failure in rock extrapolated from secondary creep. Journal of Geophysical Research: Solid Earth, 2014, 119, 1942-1953.	3.4	36
158	Vertical Heterogeneity of the Shale Reservoir in the Lower Silurian Longmaxi Formation: Analogy between the Southeastern and Northeastern Sichuan Basin, SW China. Minerals (Basel, Switzerland), 2017, 7, 151.	2.0	36
159	Micro-scale investigation on coupling of gas diffusion and mechanical deformation of shale. Journal of Petroleum Science and Engineering, 2019, 175, 961-970.	4.2	36
160	Controlling effects of differential swelling index on evolution of coal permeability. Journal of Rock Mechanics and Geotechnical Engineering, 2020, 12, 461-472.	8.1	36
161	Geodetic constraints on the shallow magma system at Soufrière Hills Volcano, Montserrat. Geophysical Research Letters, 2005, 32, .	4.0	35
162	Influence of extrusion rate and magma rheology on the growth of lava domes: Insights from particle-dynamics modeling. Journal of Volcanology and Geothermal Research, 2014, 285, 100-117.	2.1	35

#	Article	IF	CITATIONS
163	Poreâ€Scale Reconstruction and Simulation of Nonâ€Darcy Flow in Synthetic Porous Rocks. Journal of Geophysical Research: Solid Earth, 2018, 123, 2770-2786.	3.4	35
164	Permeability evolution and crack characteristics in granite under treatment at high temperature. International Journal of Rock Mechanics and Minings Sciences, 2020, 134, 104461.	5.8	35
165	Application of non-linear flow laws in determining rock fissure geometry from single borehole pumping tests. International Journal of Rock Mechanics and Mining Sciences, 1986, 23, 245-254.	0.0	34
166	Stress-dependent flow through fractured clay till: a laboratory study. Canadian Geotechnical Journal, 1996, 33, 449-457.	2.8	34
167	Permeability evolution in carbonate fractures: Competing roles of confining stress and fluid pH. Water Resources Research, 2013, 49, 2828-2842.	4.2	34
168	Multidomain Two-Phase Flow Model to Study the Impacts of Hydraulic Fracturing on Shale Gas Production. Energy & Fuels, 2020, 34, 4273-4288.	5.1	34
169	Dislocation Analysis of Penetration in Saturated Porous Media. Journal of Engineering Mechanics - ASCE, 1991, 117, 391-408.	2.9	33
170	Analysis of Piezocone Dissipation Data Using Dislocation Methods. Journal of Geotechcnical Engineering, 1993, 119, 1601-1623.	0.4	33
171	Quantitative Analysis of Nanopore Structural Characteristics of Lower Paleozoic Shale, Chongqing (Southwestern China): Combining FIB-SEM and NMR Cryoporometry. Energy & Fuels, 2017, 31, 13317-13328.	5.1	33
172	A suite of benchmark and challenge problems for enhanced geothermal systems. Geomechanics and Geophysics for Geo-Energy and Geo-Resources, 2018, 4, 79-117.	2.9	33
173	Friction of Longmaxi Shale Gouges and Implications for Seismicity During Hydraulic Fracturing. Journal of Geophysical Research: Solid Earth, 2020, 125, e2020JB019885.	3.4	33
174	Utilization of carbon dioxide from coal-based power plants as a heat transfer fluid for electricity generation in enhanced geothermal systems (EGS). Energy, 2013, 57, 505-512.	8.8	32
175	Evaluation and modeling of water vapor sorption and transport in nanoporous shale. International Journal of Coal Geology, 2020, 228, 103553.	5.0	32
176	Dynamic fluid interactions during CO2-ECBM and CO2 sequestration in coal seams. Part 2: CO2-H2O wettability. Fuel, 2020, 279, 118560.	6.4	32
177	A fracture mapping and extended finite element scheme for coupled deformation and fluid flow in fractured porous media. International Journal for Numerical and Analytical Methods in Geomechanics, 2013, 37, 2916-2936.	3.3	31
178	Influence of weakening minerals on ensemble strength and slip stability of faults. Journal of Geophysical Research: Solid Earth, 2017, 122, 7090-7110.	3.4	31
179	Triple-Porosity Modelling for the Simulation of Multiscale Flow Mechanisms in Shale Reservoirs. Geofluids, 2018, 2018, 1-11.	0.7	31
180	Airflow disturbance induced by coal mine outburst shock waves: A case study of a gas outburst disaster in China. International Journal of Rock Mechanics and Minings Sciences, 2020, 128, 104262.	5.8	31

#	Article	IF	CITATIONS
181	Reservoir stimulation and induced seismicity: Roles of fluid pressure and thermal transients on reactivated fractured networks. Geothermics, 2014, 51, 368-379.	3.4	30
182	Seismicity-permeability coupling in the behavior of gas shales, CO2 storage and deep geothermal energy. Geomechanics and Geophysics for Geo-Energy and Geo-Resources, 2017, 3, 189-198.	2.9	30
183	The Role of Mineral Composition on the Frictional and Stability Properties of Powdered Reservoir Rocks. Journal of Geophysical Research: Solid Earth, 2019, 124, 1480-1497.	3.4	30
184	Monitoring oil displacement and CO2 trapping in low-permeability media using NMR: A comparison of miscible and immiscible flooding. Fuel, 2021, 305, 121606.	6.4	30
185	Poromechanical response of fractured-porous rock masses. Journal of Petroleum Science and Engineering, 1995, 13, 155-168.	4.2	29
186	Permeability Determination from On-the-Fly Piezocone Sounding. Journal of Geotechnical and Geoenvironmental Engineering - ASCE, 2005, 131, 643-653.	3.0	29
187	Tracer transport in a fractured chalk: X-ray CT characterization and digital-image-based (DIB) simulation. Transport in Porous Media, 2007, 70, 25-42.	2.6	29
188	Interactions and exchange of CO2 and H2O in coals: an investigation by low-field NMR relaxation. Scientific Reports, 2016, 6, 19919.	3.3	29
189	Preliminary study on the feasibility of co-exploitation of coal and uranium. International Journal of Rock Mechanics and Minings Sciences, 2019, 123, 104098.	5.8	29
190	Evolution of Shale Permeability under the Influence of Gas Diffusion from the Fracture Wall into the Matrix. Energy & Fuels, 2020, 34, 4393-4406.	5.1	29
191	Anomalous distribution of microearthquakes in the Newberry Geothermal Reservoir: Mechanisms and implications. Geothermics, 2016, 63, 62-73.	3.4	28
192	Key strata characteristics controlling the integrity of deep wells in longwall mining areas. International Journal of Coal Geology, 2017, 172, 31-42.	5.0	28
193	Predicting fugitive gas emissions from gob-to-face in longwall coal mines: Coupled analytical and numerical modeling. International Journal of Heat and Mass Transfer, 2020, 150, 119392.	4.8	28
194	Influence of fracture roughness on shear strength, slip stability and permeability: A mechanistic analysis by three-dimensional digital rock modeling. Journal of Rock Mechanics and Geotechnical Engineering, 2020, 12, 720-731.	8.1	28
195	Response of submarine hydrologic monitoring instruments to formation pressure changes: Theory and application to Nankai advanced CORKs. Journal of Geophysical Research, 2008, 113, .	3.3	27
196	Dual reservoir structure at Soufrière Hills Volcano inferred from continuous GPS observations and heterogeneous elastic modeling. Geophysical Research Letters, 2010, 37, .	4.0	27
197	Shale Pore Characterization Using NMR Cryoporometry with Octamethylcyclotetrasiloxane as the Probe Liquid. Energy & Fuels, 2017, 31, 6951-6959.	5.1	27
198	A novel pore size classification method of coals: Investigation based on NMR relaxation. Journal of Natural Gas Science and Engineering, 2020, 81, 103466.	4.4	27

#	Article	IF	CITATIONS
199	Shale gas reservoir modeling and production evaluation considering complex gas transport mechanisms and dispersed distribution of kerogen. Petroleum Science, 2021, 18, 195-218.	4.9	27
200	Prototype PBO instrumentation of CALIPSO project captures world-record lava dome collapse on Montserrat Volcano. Eos, 2004, 85, 317.	0.1	26
201	Spontaneous Switching between Permeability Enhancement and Degradation in Fractures in Carbonate: Lumped Parameter Representation of Mechanically- and Chemically-Mediated Dissolution. Transport in Porous Media, 2006, 65, 385-409.	2.6	26
202	Types, characteristics and effects of natural fluid pressure fractures in shale: A case study of the Paleogene strata in Eastern China. Petroleum Exploration and Development, 2016, 43, 634-643.	7.0	26
203	Experimental observations of heterogeneous strains inside a dual porosity sample under the influence of gas-sorption: A case study of fractured coal. International Journal of Coal Geology, 2020, 223, 103450.	5.0	26
204	The mechanics of harmonic gas pressurization and failure of lavaÂdomes. Geophysical Journal International, 2001, 145, 187-198.	2.4	25
205	Modeling the CO2-based enhanced geothermal system (EGS) paired with integrated gasification combined cycle (IGCC) for symbiotic integration of carbon dioxide sequestration with geothermal heat utilization. International Journal of Greenhouse Gas Control, 2015, 32, 197-212.	4.6	25
206	Stress redistribution and fracture propagation during restimulation of gas shale reservoirs. Journal of Petroleum Science and Engineering, 2017, 154, 150-160.	4.2	25
207	Characterization of Swelling Modulus and Effective Stress Coefficient Accommodating Sorption-Induced Swelling in Coal. Energy & Fuels, 2017, 31, 8843-8851.	5.1	25
208	Controls of hydrocarbon generation on the development of expulsion fractures in organic-rich shale: Based on the Paleogene Shahejie Formation in the Jiyang Depression, Bohai Bay Basin, East China. Marine and Petroleum Geology, 2017, 86, 1406-1416.	3.3	25
209	The Impact of Frictional Healing on Stickâ€Slip Recurrence Interval and Stress Drop: Implications for Earthquake Scaling. Journal of Geophysical Research: Solid Earth, 2017, 122, 10,102.	3.4	25
210	Hydraulic fracturing for improved nutrient delivery in microbially-enhanced coalbed-methane (MECBM) production. Journal of Natural Gas Science and Engineering, 2018, 60, 294-311.	4.4	25
211	Impact of shale matrix mechanical interactions on gas transport during production. Journal of Petroleum Science and Engineering, 2020, 184, 106524.	4.2	25
212	The influence of particle morphology on microbially induced CaCO ₃ clogging in granular media. Marine Georesources and Geotechnology, 2021, 39, 74-81.	2.1	25
213	Analytical models for flow through obstructed domains. Journal of Geophysical Research, 1992, 97, 2085-2093.	3.3	24
214	Constraints on compaction rate and equilibrium in the pressure solution creep of quartz aggregates and fractures: Controls of aqueous concentration. Journal of Geophysical Research, 2010, 115, .	3.3	24
215	Influence of dilatancy on the frictional constitutive behavior of a saturated fault zone under a variety of drainage conditions. Journal of Geophysical Research, 2011, 116, .	3.3	24
216	The Impact of Oriented Perforations on Fracture Propagation and Complexity in Hydraulic Fracturing. Processes, 2018, 6, 213.	2.8	24

#	Article	IF	CITATIONS
217	Long-Term Evolution of Coal Permeability Under Effective Stresses Gap Between Matrix and Fracture During CO2 Injection. Transport in Porous Media, 2019, 130, 969-983.	2.6	24
218	Fracture penetration and proppant transport in gas- and foam-fracturing. Journal of Natural Gas Science and Engineering, 2020, 77, 103269.	4.4	24
219	Ridgecrest aftershocks at Coso suppressed by thermal destressing. Nature, 2021, 595, 70-74.	27.8	24
220	Limits in determining permeability from on-the-fly uCPT sounding. Geotechnique, 2007, 57, 679-685.	4.0	23
221	Thermal drawdown and lateâ€stage seismicâ€slip fault reactivation in enhanced geothermal reservoirs. Journal of Geophysical Research: Solid Earth, 2014, 119, 8936-8949.	3.4	23
222	Changes in pore structure of coal caused by coal-to-gas bioconversion. Scientific Reports, 2017, 7, 3840.	3.3	23
223	Theory of dike intrusion in a saturated porous solid. Journal of Geophysical Research, 1992, 97, 9105-9117.	3.3	22
224	Explosion dynamics from strainmeter and microbarometer observations, Soufrière Hills Volcano, Montserrat: 2008–2009. Geophysical Research Letters, 2010, 37, .	4.0	22
225	Evolution of the transport properties of fractures subject to thermally and mechanically activated mineral alteration and redistribution. Geofluids, 2016, 16, 396-407.	0.7	22
226	Experimental Investigation on the Mechanical Behavior of Victorian Brown Coal under Brine Saturation. Energy & amp; Fuels, 2018, 32, 5799-5811.	5.1	22
227	The effects of mineral distribution, pore geometry, and pore density on permeability evolution in gas shales. Fuel, 2019, 257, 116005.	6.4	22
228	W-shaped permeability evolution of coal with supercritical CO2 phase transition. International Journal of Coal Geology, 2019, 211, 103221.	5.0	22
229	Slip Velocity Dependence of Friction-Permeability Response of Shale Fractures. Rock Mechanics and Rock Engineering, 2020, 53, 2109-2121.	5.4	22
230	Near-source characteristics of two-phase gas–solid outbursts in roadways. International Journal of Coal Science and Technology, 2021, 8, 685-696.	6.0	22
231	Effective application of proppants during the hydraulic fracturing of coal seam gas reservoirs: Implications from laboratory testings of propped and unpropped coal fractures. Fuel, 2021, 304, 121394.	6.4	22
232	A reduced degree of freedom model for thermal permeability enhancement in blocky rock. Geothermics, 1989, 18, 691-709.	3.4	21
233	Classification and idealized limit-equilibrium analyses of dome collapses at Soufrière Hills volcano, Montserrat, during growth of the first lava dome: November 1995–March 1998. Journal of Volcanology and Geothermal Research, 2005, 139, 241-258.	2.1	21
234	Dissolution-induced preferential flow in a limestone fracture. Journal of Contaminant Hydrology, 2005, 78, 53-70.	3.3	21

#	Article	IF	CITATIONS
235	Permeability Evolution of Propped Artificial Fractures in Green River Shale. Rock Mechanics and Rock Engineering, 2017, 50, 1473-1485.	5.4	21
236	An accelerating precursor to predict "time-to-failure―in creep and volcanic eruptions. Journal of Volcanology and Geothermal Research, 2017, 343, 252-262.	2.1	21
237	Coalbed methane reservoir fracture evaluation through the novel passive microseismic survey and its implications on permeable and gas production. Journal of Natural Gas Science and Engineering, 2020, 76, 103181.	4.4	21
238	Mechanisms for rainfall-concurrent lava dome collapses at Soufrière Hills Volcano, 2000–2002. Journal of Volcanology and Geothermal Research, 2007, 160, 195-209.	2.1	20
239	Hydrogeology of the vicinity of Homestake mine, South Dakota, USA. Hydrogeology Journal, 2012, 20, 27-43.	2.1	20
240	Reservoir permeability mapping using microearthquake data. Geothermics, 2018, 72, 83-100.	3.4	20
241	Influencing factors and fracability of lacustrine shale oil reservoirs. Marine and Petroleum Geology, 2019, 110, 463-471.	3.3	20
242	Anisotropy of acoustic emission in coal under the uniaxial loading condition. Chaos, Solitons and Fractals, 2020, 130, 109465.	5.1	20
243	Analytical solutions for multi-stage fractured shale gas reservoirs with damaged fractures and stimulated reservoir volumes. Journal of Petroleum Science and Engineering, 2020, 187, 106686.	4.2	20
244	Dynamic Fluid Interactions during CO ₂ -Enhanced Coalbed Methane and CO ₂ Sequestration in Coal Seams. Part 1: CO ₂ –CH ₄ Interactions. Energy & Fuels, 2020, 34, 8274-8282.	5.1	20
245	Constraining maximum event magnitude during injection-triggered seismicity. Nature Communications, 2021, 12, 1528.	12.8	20
246	Hydro-mechanical-chemical modeling of sub-nanopore capillary-confinement on CO2-CCUS-EOR. Energy, 2021, 225, 120203.	8.8	20
247	A boundary elementâ€finite element procedure for porous and fractured media flow. Water Resources Research, 1987, 23, 551-560.	4.2	19
248	Evaluation of pore water pressure fluctuation around an advancing longwall face. Advances in Water Resources, 1999, 22, 633-644.	3.8	19
249	Numerical simulation of two-phase flow in deformable porous media: Application to carbon dioxide storage in the subsurface. Mathematics and Computers in Simulation, 2012, 82, 1919-1935.	4.4	19
250	Evolution of Strength and Permeability in Stressed Fractures with Fluid–Rock Interactions. Pure and Applied Geophysics, 2016, 173, 525-536.	1.9	19
251	Coupled Thermo-Hydro-Mechanical-Chemical Modeling of Permeability Evolution in a CO ₂ -Circulated Geothermal Reservoir. Geofluids, 2019, 2019, 1-15.	0.7	19
252	Dynamic Stressing of Naturally Fractured Rocks: On the Relation Between Transient Changes in Permeability and Elastic Wave Velocity. Geophysical Research Letters, 2020, 47, e2019GL083557.	4.0	19

#	Article	IF	CITATIONS
253	Review of fundamental studies of CO2 fracturing: Fracture propagation, propping and permeating. Journal of Petroleum Science and Engineering, 2021, 205, 108823.	4.2	19
254	Contribution of thermal expansion on gas adsorption to coal sorption-induced swelling. Chemical Engineering Journal, 2022, 432, 134427.	12.7	19
255	Theory of thermal recovery from a spherically stimulated hot dry rock reservoir. Journal of Geophysical Research, 1989, 94, 1927-1934.	3.3	18
256	Mechanical and transport constitutive models for fractures subject to dissolution and precipitation. International Journal for Numerical and Analytical Methods in Geomechanics, 2010, 34, 533-549.	3.3	18
257	A dynamic-pulse pseudo-pressure method to determine shale matrix permeability at representative reservoir conditions. International Journal of Coal Geology, 2018, 193, 61-72.	5.0	18
258	Cyclic Permeability Evolution During Repose Then Reactivation of Fractures and Faults. Journal of Geophysical Research: Solid Earth, 2019, 124, 4492-4506.	3.4	18
259	The transition from steady frictional sliding to inertia-dominated instability with rate and state friction. Journal of the Mechanics and Physics of Solids, 2019, 122, 116-125.	4.8	18
260	Coupled multiscale-modeling of microwave-heating-induced fracturing in shales. International Journal of Rock Mechanics and Minings Sciences, 2020, 136, 104520.	5.8	18
261	Impact of equilibration time lag between matrix and fractures on the evolution of coal permeability. Fuel, 2021, 290, 120029.	6.4	18
262	Compressive Strength of MICP-Treated Silica Sand with Different Particle Morphologies and Gradings. Geomicrobiology Journal, 2022, 39, 148-154.	2.0	18
263	Modeling Contaminant Migration with Linear Sorption in Strongly Heterogeneous Media. Journal of Environmental Engineering, ASCE, 1997, 123, 1116-1125.	1.4	17
264	Instability of exogenous lava lobes during intense rainfall. Bulletin of Volcanology, 2004, 66, 725-734.	3.0	17
265	Unique strainmeter observations of Vulcanian explosions, Soufrière Hills Volcano, Montserrat, July 2003. Geophysical Research Letters, 2010, 37, .	4.0	17
266	Experimental Measurements of Stress and Chemical Controls on the Evolution of Fracture Permeability. Transport in Porous Media, 2013, 98, 15-34.	2.6	17
267	Strengthening mylonitized soft-coal reservoirs by microbial mineralization. International Journal of Coal Geology, 2018, 200, 166-172.	5.0	17
268	Organic Geochemical and Petrographic Characteristics of the Coal Measure Source Rocks of Pinghu Formation in the Xihu Sag of the East China Sea Shelf Basin: Implications for Coal Measure Gas Potential. Acta Geologica Sinica, 2020, 94, 364-375.	1.4	17
269	Effect of adsorption-induced matrix swelling on coal permeability evolution of micro-fracture with the real geometry. Petroleum Science, 2021, 18, 1143-1152.	4.9	17
270	Physical and numerical studies of a fracture system model. Water Resources Research, 1989, 25, 457-462.	4.2	16

#	Article	IF	CITATIONS
271	Finite element analysis of the modified ring test for determining mode I fracture toughness. International Journal of Rock Mechanics and Mining Sciences, 1996, 33, 1-15.	0.0	16
272	Short-Timescale Chemo-Mechanical Effects and their Influence on the Transport Properties of Fractured Rock. Pure and Applied Geophysics, 2006, 163, 2051-2070.	1.9	16
273	Topographic influence on stability for gas wells penetrating longwall mining areas. International Journal of Coal Geology, 2014, 132, 23-36.	5.0	16
274	Controls of natural fractures on the texture of hydraulic fractures in rock. Journal of Petroleum Science and Engineering, 2018, 165, 616-626.	4.2	16
275	Temperature and Fluid Pressurization Effects on Frictional Stability of Shale Faults Reactivated by Hydraulic Fracturing in the Changning Block, Southwest China. Journal of Geophysical Research: Solid Earth, 2020, 125, e2020JB019584.	3.4	16
276	Continuous Compaction and Permeability Evolution in Longwall Gob Materials. Rock Mechanics and Rock Engineering, 2020, 53, 5489-5510.	5.4	16
277	The Potential for Lowâ€Grade Metamorphism to Facilitate Fault Instability in a Geothermal Reservoir. Geophysical Research Letters, 2021, 48, e2021GL093552.	4.0	16
278	A comparative evaluation of the parallel flow and spherical reservoir models of HDR geothermal systems. Journal of Volcanology and Geothermal Research, 1990, 44, 283-293.	2.1	15
279	Numerical modeling of stress-dependent permeability. International Journal of Rock Mechanics and Minings Sciences, 1997, 34, 2.e1-2.e14.	5.8	15
280	Strain-dependent Fluid Flow Defined Through Rock Mass Classification Schemes. Rock Mechanics and Rock Engineering, 2000, 33, 75-92.	5.4	15
281	Evolution of Friction and Permeability in a Propped Fracture under Shear. Geofluids, 2017, 2017, 1-13.	0.7	15
282	Collapse of Reacted Fracture Surface Decreases Permeability and Frictional Strength. Journal of Geophysical Research: Solid Earth, 2019, 124, 12799-12811.	3.4	15
283	Pore-Scale Water Vapor Condensation Behaviors in Shales: An Experimental Study. Transport in Porous Media, 2020, 135, 713-734.	2.6	15
284	A two-stage step-wise framework for fast optimization of well placement in coalbed methane reservoirs. International Journal of Coal Geology, 2020, 225, 103479.	5.0	15
285	Permeable rock matrix sealed with microbially-induced calcium carbonate precipitation: Evolutions of mechanical behaviors and associated microstructure. Engineering Geology, 2022, 304, 106697.	6.3	15
286	A critical review of coal permeability models. Fuel, 2022, 326, 125124.	6.4	15
287	A phenomenological failure criterion for brittle rock. Rock Mechanics and Rock Engineering, 1991, 24, 133-153.	5.4	14
288	Pore-pressure response due to penetration through layered media. International Journal for Numerical and Analytical Methods in Geomechanics, 1992, 16, 45-64.	3.3	14

#	Article	IF	CITATIONS
289	Magmatic-metering controls the stopping and restarting of eruptions. Geophysical Research Letters, 2011, 38, n/a-n/a.	4.0	14
290	The effects of thermal stress and fluid pressure on induced seismicity during stimulation to production within fractured reservoirs. Terra Nova, 2013, 25, 374-380.	2.1	14
291	Reach and geometry of dynamic gas-driven fractures. International Journal of Rock Mechanics and Minings Sciences, 2020, 129, 104287.	5.8	14
292	Vertical heterogeneity of permeability and gas content of ultra-high-thickness coalbed methane reservoirs in the southern margin of the Junggar Basin and its influence on gas production. Journal of Natural Gas Science and Engineering, 2020, 81, 103455.	4.4	14
293	Experimental study on the feasibility of microwave heating fracturing for enhanced shale gas recovery. Journal of Natural Gas Science and Engineering, 2021, 94, 104073.	4.4	14
294	The use of supercritical CO2 in deep geothermal reservoirs as a working fluid: Insights from coupled THMC modeling. International Journal of Rock Mechanics and Minings Sciences, 2021, 147, 104872.	5.8	14
295	A critical analysis of shale laboratory permeability evolution data. Energy, 2021, 236, 121405.	8.8	14
296	Shale gas production from reservoirs with hierarchical multiscale structural heterogeneities. Journal of Petroleum Science and Engineering, 2022, 208, 109380.	4.2	14
297	A grain texture model to investigate effects of grain shape and orientation on macro-mechanical behavior of crystalline rock. International Journal of Rock Mechanics and Minings Sciences, 2021, 148, 104971.	5.8	14
298	Indentation of a sharp penetrometer in a poroelastic medium. International Journal of Solids and Structures, 1998, 35, 4895-4904.	2.7	13
299	Laboratory investigation of the frictional behavior of granular volcanic material. Journal of Volcanology and Geothermal Research, 2008, 173, 265-279.	2.1	13
300	Three-Dimensional Numerical Modeling of Grain-Scale Mechanical Behavior of Sandstone Containing an Inclined Rough Joint. Rock Mechanics and Rock Engineering, 2021, 54, 905-919.	5.4	13
301	Stress perturbation caused by multistage hydraulic fracturing: Implications for deep fault reactivation. International Journal of Rock Mechanics and Minings Sciences, 2021, 141, 104704.	5.8	13
302	Wedge stability in the roof of a circular tunnel: Plane strain condition. International Journal of Rock Mechanics and Mining Sciences, 1986, 23, 177-181.	0.0	12
303	Topographic Influence of Longwall Mining on Ground-Water Supplies. Ground Water, 1995, 33, 786-793.	1.3	12
304	Hydraulic Conductivity Measurement from On-the-Fly uCPT Sounding and from VisCPT. Journal of Geotechnical and Geoenvironmental Engineering - ASCE, 2008, 134, 1720-1729.	3.0	12
305	Geodetic imaging of thermal deformation in geothermal reservoirs - production, depletion and fault reactivation. Journal of Volcanology and Geothermal Research, 2017, 338, 79-91.	2.1	12
306	Influence of conduit flow mechanics on magma rheology and the growth style of lava domes. Geophysical Journal International, 2018, 213, 1768-1784.	2.4	12

#	Article	IF	CITATIONS
307	Swelling and embedment induced by sub- and super-critical-CO2 on the permeability of propped fractures in shale. International Journal of Coal Geology, 2020, 225, 103496.	5.0	12
308	Evolution and analysis of gas sorption-induced coal fracture strain data. Petroleum Science, 2020, 17, 376-392.	4.9	12
309	The 1980 pressure response and flank failure of Mount St. Helens (USA) inferred from seismic scaling exponents. Journal of Volcanology and Geothermal Research, 2005, 144, 155-168.	2.1	11
310	Permeability Evolution of Pyrolytically-Fractured Oil Shale under In Situ Conditions. Energies, 2018, 11, 3033.	3.1	11
311	A strain based approach to calculate disparities in pore structure between shale basins during permeability evolution. Journal of Natural Gas Science and Engineering, 2019, 68, 102893.	4.4	11
312	Determination of the critical flow pore diameter of shale caprock. Marine and Petroleum Geology, 2020, 112, 104042.	3.3	11
313	Controlling Induced Earthquake Magnitude by Cycled Fluid Injection. Geophysical Research Letters, 2021, 48, e2021GL092885.	4.0	11
314	Microstructure characterization of kerogen in mature shale: Molecular investigation of micropore development. Journal of Natural Gas Science and Engineering, 2021, 95, 104239.	4.4	11
315	Long-term effect of desorption-induced matrix shrinkage on the evolution of coal permeability during coalbed methane production. Journal of Petroleum Science and Engineering, 2022, 208, 109378.	4.2	11
316	Micro-fractures in coal induced by high pressure CO2 gas fracturing. Fuel, 2022, 311, 122148.	6.4	11
317	Transient poroelastic response of equivalent porous media over a mining panel. Engineering Geology, 1993, 35, 49-64.	6.3	10
318	Experimental Observations of Gas-sorption-Induced Strain Gradients and their Implications on Permeability Evolution of Shale. Rock Mechanics and Rock Engineering, 2021, 54, 3927-3943.	5.4	10
319	Mechanisms of tripartite permeability evolution for supercritical CO2 in propped shale fractures. Fuel, 2021, 292, 120188.	6.4	10
320	Rapid gas desorption and its impact on gas-coal outbursts as two-phase flows. Chemical Engineering Research and Design, 2021, 150, 478-488.	5.6	10
321	Theory of Partially Drained Piezometer Insertion. Journal of Geotechcnical Engineering, 1990, 116, 899-914.	0.4	9
322	On the modeling of miscible flow in multi-component porous media. Transport in Porous Media, 1995, 21, 19-46.	2.6	9
323	Evolution of permeability in heterogeneous granular aggregates during chemical compaction: Granular mechanics models. Journal of Geophysical Research, 2012, 117, .	3.3	9
324	Strength evolution in heterogeneous granular aggregates during chemo–mechanical compaction. International Journal of Rock Mechanics and Minings Sciences, 2013, 60, 217-226.	5.8	9

#	Article	IF	CITATIONS
325	Dynamic impacts on the survivability of shale gas wells piercing longwall panels. Journal of Natural Gas Science and Engineering, 2015, 26, 1130-1147.	4.4	9
326	Conceptual model and numerical analysis of the Desert Peak EGS project: Reservoir response to the shallow medium flow-rate hydraulic stimulation phase. Geothermics, 2016, 63, 139-156.	3.4	9
327	A Gaussian Decomposition Method and its applications to the prediction of shale gas production. Fuel, 2018, 224, 331-347.	6.4	9
328	Does Lowâ€Viscosity Fracturing Fluid Always Create Complex Fractures?. Journal of Geophysical Research: Solid Earth, 2020, 125, e2020JB020332.	3.4	9
329	Gas permeability and fracture compressibility for proppant-supported shale fractures under high stress. Journal of Natural Gas Science and Engineering, 2021, 95, 104157.	4.4	9
330	A fully coupled multidomain and multiphysics model considering stimulation patterns and thermal effects for evaluation of coalbed methane (CBM) extraction. Journal of Petroleum Science and Engineering, 2022, 214, 110506.	4.2	9
331	Evaluation of the post-mining groundwater regime following longwall mining. Hydrological Processes, 1997, 11, 1945-1961.	2.6	8
332	The Evolution of Permeability in Natural Fractures – the Competing Roles of Pressure Solution and Free-Face Dissolution. Elsevier Geo-Engineering Book Series, 2004, , 721-726.	0.0	8
333	Application of Composite Indices for Improving Joint Detection Capabilities of Instrumented Roof Bolt Drills in Underground Mining and Construction. Rock Mechanics and Rock Engineering, 2018, 51, 849-860.	5.4	8
334	Relationships between mechanical and transport properties in Marcellus shale. International Journal of Rock Mechanics and Minings Sciences, 2019, 119, 205-210.	5.8	8
335	Statistical Analysis of the CapabilitiesÂof Various Pattern Recognition Algorithms for FractureÂDetection Based on Monitoring Drilling Parameters. Rock Mechanics and Rock Engineering, 2020, 53, 2265-2278.	5.4	8
336	Microbially Induced Calcium Carbonate Plugging for Enhanced Oil Recovery. Geofluids, 2020, 2020, 1-10.	0.7	8
337	Interpretation of Gas/Water Relative Permeability of Coal Using the Hybrid Bayesian-Assisted History Matching: New Insights. Energies, 2021, 14, 626.	3.1	8
338	Discrete fracture matrix modelling of fully-coupled CO2 flow – Deformation processes in fractured coal. International Journal of Rock Mechanics and Minings Sciences, 2021, 138, 104644.	5.8	8
339	Nonlinear elastodynamic behavior of intact and fractured rock under in-situ stress and saturation conditions. Journal of the Mechanics and Physics of Solids, 2021, 153, 104491.	4.8	8
340	Down-dip circulation at the united downs deep geothermal power project maximizes heat recovery and minimizes seismicity. Geothermics, 2021, 96, 102204.	3.4	8
341	Influence of water on elastic deformation of coal and its control on permeability in coalbed methane production. Journal of Petroleum Science and Engineering, 2022, 208, 109603.	4.2	8
342	Frictional Stability of Metamorphic Epidote in Granitoid Faults Under Hydrothermal Conditions and Implications for Injectionâ€Induced Seismicity. Journal of Geophysical Research: Solid Earth, 2022, 127, .	3.4	8

#	Article	IF	CITATIONS
343	Thermal recovery from a multiple stimulated HDR reservoir. Geothermics, 1989, 18, 761-774.	3.4	7
344	A Modified Gauss-Newton Method for Aquifer Parameter Identification. Ground Water, 1995, 33, 662-668.	1.3	7
345	Evolution of permeability in sand injectite systems. International Journal of Rock Mechanics and Minings Sciences, 2018, 106, 176-189.	5.8	7
346	Multiscale modeling of shock wave propagation induced by coal and gas outbursts. Chemical Engineering Research and Design, 2019, 125, 164-171.	5.6	7
347	Morphologic variation of an evolving dome controlled by the extrusion of finite yield strength magma. Journal of Volcanology and Geothermal Research, 2019, 370, 51-64.	2.1	7
348	Ensemble Shear Strength, Stability, and Permeability of Mixed Mineralogy Fault Gouge Recovered From 3D Granular Models. Journal of Geophysical Research: Solid Earth, 2019, 124, 425-441.	3.4	7
349	Creep Rupture and Permeability Evolution in High Temperature Heat-Treated Sandstone Containing Pre-Existing Twin Flaws. Energies, 2021, 14, 6362.	3.1	7
350	Water Liberating/Sealing effects on shale gas Extraction: A fully coupled multidomain and multiphysics model. Fuel, 2022, 325, 124953.	6.4	7
351	Analytical evaluation of post-excavation hydraulic conductivity field around a tunnel. International Journal of Rock Mechanics and Minings Sciences, 1997, 34, 181.e1-181.e7.	5.8	6
352	Indentation of a Free-Falling Sharp Penetrometer into a Poroelastic Seabed. Journal of Engineering Mechanics - ASCE, 2004, 130, 170-179.	2.9	6
353	Pore Pressure Response Following Undrained uCPT Sounding in a Dilating Soil. Journal of Geotechnical and Geoenvironmental Engineering - ASCE, 2006, 132, 1485-1495.	3.0	6
354	Insights from electron backscatter diffraction into the origin of fibrous calcite veins in organic-rich shale from lower Es3 to upper Es4, Jiyang Depression, China. Marine and Petroleum Geology, 2020, 113, 104131.	3.3	6
355	Impact of Nitrogen Injection on Pore Structure and Adsorption Capacity of High Volatility Bituminous Coal. Energy & Fuels, 2020, 34, 8216-8226.	5.1	6
356	Proppant embedment in coal and shale: Impacts of stress hardening and sorption. International Journal of Coal Geology, 2020, 227, 103545.	5.0	6
357	Effect of slick-water fracturing fluid on the frictional properties of shale reservoir rock gouges. Geomechanics and Geophysics for Geo-Energy and Geo-Resources, 2020, 6, 1.	2.9	6
358	Numerical simulation of mixed aseismic/seismic fault-slip induced by fluid injection using coupled X-FEM analysis. International Journal of Rock Mechanics and Minings Sciences, 2021, 147, 104871.	5.8	6
359	Immiscible/Near-Miscible relative permeability for confined fluids at high-pressure and high-temperature for a fractal reservoir. Fuel, 2022, 310, 122389.	6.4	6
360	An adaptive characteristics method for advective-diffusive transport. Applied Mathematical Modelling, 1989, 13, 682-692.	4.2	5

#	Article	IF	CITATIONS
361	Numerical modeling of stress-dependent permeability. International Journal of Rock Mechanics and Minings Sciences, 1997, 34, 135.e1-135.e14.	5.8	5
362	A coupled hydromechanical system defined through rock mass classification schemes. International Journal for Numerical and Analytical Methods in Geomechanics, 1999, 23, 1945-1960.	3.3	5
363	Mechanical Response of Lined and Unlined Heated Drifts. Rock Mechanics and Rock Engineering, 2001, 34, 201-215.	5.4	5
364	Stress Analysis of a Borehole in Saturated Rocks Under in situ Mechanical, Hydrological and Thermal Interactions. Energy Sources, Part A: Recovery, Utilization and Environmental Effects, 2007, 30, 157-169.	2.3	5
365	Evolution of the Pore-Pressure Field around a Moving Conical Penetrometer of Finite Size. Journal of Engineering Mechanics - ASCE, 2010, 136, 263-272.	2.9	5
366	Pairing Integrated Gasification and Enhanced Geothermal Systems (EGS) in Semiarid Environments. Energy & Fuels, 2012, 26, 7378-7389.	5.1	5
367	Mechanical and Transport Characteristics of Coal-Biomass Mixtures for Advanced IGCC Systems. Energy & Fuels, 2012, 26, 5729-5739.	5.1	5
368	Chapter 12 Geodetic imaging of magma migration at Soufrière Hills Volcano 1995 to 2008. Geological Society Memoir, 2014, 39, 219-227.	1.7	5
369	Chapter 15 The SEA-CALIPSO volcano imaging experiment at Montserrat: plans, campaigns at sea and on land, scientific results, and lessons learned. Geological Society Memoir, 2014, 39, 253-289.	1.7	5
370	Radial Permeability Measurements for Shale Using Variable Pressure Gradients. Acta Geologica Sinica, 2020, 94, 269-279.	1.4	5
371	The influence of fault reactivation on injection-induced dynamic triggering of permeability evolution. Geophysical Journal International, 2020, 223, 1481-1496.	2.4	5
372	Evolution of Production and Transport Characteristics of Steeply-Dipping Ultra-Thick Coalbed Methane Reservoirs. Energies, 2020, 13, 5081.	3.1	5
373	A NEW FRACTAL TEMPORAL CONDUCTIVITY MODEL FOR PROPPED FRACTURE AND ITS APPLICATION IN TIGHT RESERVOIRS. Fractals, 2020, 28, 2050074.	3.7	5
374	A model for focused-beam microwave heating on rock fracturing. Geomechanics and Geophysics for Geo-Energy and Geo-Resources, 2021, 7, 1.	2.9	5
375	Computational Methods in Fluid Flow. , 1993, , 173-189.		5
376	A transient dual porosity/permeability model for coal multiphysics. Geomechanics and Geophysics for Geo-Energy and Geo-Resources, 2022, 8, 1.	2.9	5
377	How Does CO ₂ Adsorption Alter Coal Wettability? Implications for CO ₂ Geoâ€sequestration. Journal of Geophysical Research: Solid Earth, 2022, 127, .	3.4	5
378	Influence of Well Types on Optimizing the Co-production of Gas from Coal and Tight Formations. Energy & Fuels, 2022, 36, 6736-6754.	5.1	5

#	Article	IF	CITATIONS
379	The role of permeability evolution in fault zones on the structural and hydro-mechanical characteristics of shortening basins. Marine and Petroleum Geology, 2012, 29, 143-151.	3.3	4
380	A new apparatus for the concurrent measurement of friction and permeability evolution in fault gouge. International Journal of Rock Mechanics and Minings Sciences, 2019, 121, 104046.	5.8	4
381	Effects of Heterogeneous Local Swelling and Multiple Pore Types on Coal and Shale Permeability Evolution. , 2020, , .		4
382	Coupled hydro-mechanical evolution of fracture permeability in sand injectite intrusions. Journal of Rock Mechanics and Geotechnical Engineering, 2020, 12, 742-751.	8.1	4
383	The influence of the structural distribution and hardness of mineral phases on the size and shape of rock drilling particles. Marine Georesources and Geotechnology, 2020, 38, 511-517.	2.1	4
384	Inverted U-shaped permeability enhancement due to thermally induced desorption determined from strain-based analysis of experiments on shale at constant pore pressure. Fuel, 2021, 302, 121178.	6.4	4
385	Contemporary views of slope instability on active volcanoes. , 2007, , 2-9.		4
386	Petrophysical Evaluation of Shale Gas Reservoirs: A Field Case Study of Marcellus Shale. , 2019, , .		4
387	Advances in in-situ modiï¬ e d mining by ï¬,uidization and in unconventional geomechanics. Advances in Geo-Energy Research, 2021, 5, 1-4.	6.0	4
388	An effective dual-medium approach to simulate microwave heating in strongly heterogeneous rocks. Geomechanics and Geophysics for Geo-Energy and Geo-Resources, 2021, 7, 1.	2.9	4
389	Hydraulic fracture propagation and interaction with natural fractures by coupled hydro-mechanical modeling. Geomechanics and Geophysics for Geo-Energy and Geo-Resources, 2022, 8, 1.	2.9	4
390	Evaluation of stresses and displacements induced in discretely layered media. International Journal of Rock Mechanics and Mining Sciences, 1990, 27, 23-31.	0.0	3
391	Low-order finite elements for parameter identification in groundwater flow. Applied Mathematical Modelling, 1991, 15, 256-266.	4.2	3
392	Characterization of fracture aperture by inverse analysis. Canadian Geotechnical Journal, 1993, 30, 637-646.	2.8	3
393	A Coupled Flow-Transport-Deformation Model for Underground Coal Gasification. Elsevier Geo-Engineering Book Series, 2004, , 611-616.	0.0	3
394	The evolution of pore pressure fields around standard and ball penetrometers: influence of penetration rate. International Journal for Numerical and Analytical Methods in Geomechanics, 2013, 37, 2135-2153.	3.3	3
395	Geological factors on gas entrapment mechanism and prediction of coalbed methane of the no. 6 coal seam in the Jungar coalfield, northeast Ordos Basin, China. International Journal of Oil, Gas and Coal Technology, 2014, 8, 449.	0.2	3
396	A Dynamic Fractal Permeability Model for Heterogeneous Coalbed Reservoir Considering Multiphysics and Flow Regimes. , 2019, , .		3

#	Article	IF	CITATIONS
397	Failure Behavior of Hot-Dry-Rock (HDR) in Enhanced Geothermal Systems: Macro to Micro Scale Effects. Geofluids, 2020, 2020, 1-13.	0.7	3
398	Numerical Simulation of An In-situ Fluid Injection Experiment into a Fault Using Coupled X-FEM Analysis. Rock Mechanics and Rock Engineering, 2021, 54, 1027-1053.	5.4	3
399	Experimental Investigation of Elastodynamic Nonlinear Response of Dry Intact, Fractured and Saturated Rock. Rock Mechanics and Rock Engineering, 2022, 55, 2665-2678.	5.4	3
400	Non-monotonic precursory signals to multi-scale catastrophic failures. International Journal of Fracture, 2020, 226, 233-242.	2.2	3
401	Heat and mass transfer around an advancing penetrometer. International Journal of Heat and Mass Transfer, 1991, 34, 1407-1416.	4.8	2
402	Direct and integration methods of parameter estimation in groundwater transport systems. Applied Mathematical Modelling, 1992, 16, 404-413.	4.2	2
403	Parameter identification of nonsteady groundwater flow systems. Advances in Water Resources, 1992, 15, 259-269.	3.8	2
404	Displacement of formation fluids by hydraulic fracturing. Geotechnique, 1996, 46, 671-681.	4.0	2
405	Indentation of a free-falling lance penetrometer into a poroelastic seabed. International Journal for Numerical and Analytical Methods in Geomechanics, 2005, 29, 141-162.	3.3	2
406	Characterization of Hydraulic Fracture with Inflated Dislocation Moving Within a Semi-infinite Medium. Mining Science and Technology, 2007, 17, 220-225.	0.8	2
407	Topographic influence on stability for gas wells penetrating longwall mining areas. International Journal of Coal Geology, 2014, 131, 23.	5.0	2
408	Influence of Stratigraphic Conditions on the Deformation Characteristics of Oil/Gas Wells Piercing Longwall Pillars and Mining Optimization. Energies, 2017, 10, 775.	3.1	2
409	Magnitude and variation of the critical power law exponent and its physical controls. Physica A: Statistical Mechanics and Its Applications, 2018, 510, 552-557.	2.6	2
410	Mechanistic Analysis of Shale Permeability Evolution Data. , 2019, , .		2
411	A new approach to evaluate the particle size distribution from rock drilling: double peak characteristic analysis. Geomechanics and Geophysics for Geo-Energy and Geo-Resources, 2020, 6, 1.	2.9	2
412	High-resolution characterization of nanoparticle transport in heterogeneous porous media via low-field nuclear magnetic resonance. Journal of Hydrology, 2020, 583, 124558.	5.4	2
413	Imaging Elastodynamic and Hydraulic Properties of In Situ Fractured Rock: An Experimental Investigation Exploring Effects of Dynamic Stressing and Shearing. Journal of Geophysical Research: Solid Earth, 2021, 126, e2020JB021521.	3.4	2
414	MODELING THE EFFECTS OF LONGWALL MINING ON THE GROUND WATER SYSTEM. Journal of the American Society of Mining and Reclamation, 1996, 1996, 96-114.	0.3	2

#	Article	IF	CITATIONS
415	Conductivity Evolution in Propped Fractures During Reservoir Drawdown. Rock Mechanics and Rock Engineering, 2022, 55, 3583-3597.	5.4	2
416	Sorptive permeability loss determined from strain-based analysis of tightly constrained experiments on shale. Journal of Petroleum Science and Engineering, 2022, 214, 110502.	4.2	2
417	Numerical modeling of stress-dependent permeability. International Journal of Rock Mechanics and Minings Sciences, 1997, 34, 39.e1-39.e14.	5.8	1
418	Numerical modeling of stress-dependent permeability. International Journal of Rock Mechanics and Minings Sciences, 1997, 34, 44.e1-44.e14.	5.8	1
419	Vaporization-Induced Overpressures as a Trigger for the Hazardous Collapse of Lava Domes. Elsevier Geo-Engineering Book Series, 2004, 2, 709-714.	0.0	1
420	Determination of Shale Matrix Permeability through Dynamic Methane Production Experiments Using Variable Pressure Gradients. , 2018, , .		1
421	Petrophysics and Fluid Transport in Shales and Tight Reservoirs. Geofluids, 2018, 2018, 1-3.	0.7	1
422	Radial Permeability Measurement for Shale Using Variable Pressure Gradients. , 2018, , .		1
423	Induced Seismicity and Permeability Evolution in Gas Shales, CO2 Storage and Deep Geothermal Energy. , 2018, , 1-20.		1
424	The Role of Rock Mechanics in the 21st Century. Springer Series in Geomechanics and Geoengineering, 2019, , 319-357.	0.1	1
425	Poroelastic Response Resulting from Magma Intrusion. Solid Mechanics and Its Applications, 1996, , 215-233.	0.2	1
426	Some Approaches to Determine the Potential Influence of Longwall Mining on Ground Water Resources. Journal of the American Society of Mining and Reclamation, 1994, 1994, 172-179.	0.3	1
427	Laboratory Investigation of Impact of Slickwater Composition on Multiphase Permeability Evolution in Tight Sandstones. SPE Production and Operations, 2021, , 1-15.	0.6	1
428	Boundary Element Analysis in Computational Fracture Mechanics (T. A. Cruse). SIAM Review, 1989, 31, 692-692.	9.5	0
429	Some THMC Controls on the Evolution of Fracture Permeability. Elsevier Geo-Engineering Book Series, 2004, , 63-71.	0.0	0
430	Penetration-Induced Pore Pressure Magnitudes – Methods to Determine Transport Parameters from Terrestrial and Marine Penetrometer Testing. Elsevier Geo-Engineering Book Series, 2004, 2, 477-482.	0.0	0
431	Compaction and Diagenesis of Sandstones – the Role of Pressure Solution. Elsevier Geo-Engineering Book Series, 2004, 2, 733-738.	0.0	0
432	Liquefaction Resistance Recovered From "On-the-Fly" CPTu-Measured Pore Pressures. , 2008, , .		0

#	Article	IF	CITATIONS
433	The Study of Permeability Revolution in Coal Reservoir during Methane Production. Applied Mechanics and Materials, 2011, 148-149, 1491-1499.	0.2	0
434	G4: inaugural editorial. Geomechanics and Geophysics for Geo-Energy and Geo-Resources, 2015, 1, 1-2.	2.9	0
435	Evolution of Permeability in Sand Injectite Systems. , 2018, , .		0
436	Heat Transfer in Enhanced Geothermal Systems: Thermal-Hydro-Mechanical Coupled Modeling. , 2019, , 201-215.		0
437	Permeability Enhancement in Gas Shale Due to Nitrogen Flooding. , 2019, , .		0
438	The influence of CO2-transformed iron oxide grain coatings on the frictional stability and transport properties of simulated faults in sandstones. Geomechanics and Geophysics for Geo-Energy and Geo-Resources, 2020, 6, 1.	2.9	0
439	A New Coupled Geomechanical-Chemical Model for CO2 Foam Flooding and Storage in Tight Reservoir. , 2020, , .		0
440	Mechanisms of fluid overpressurization related to instability of slopes on active volcanoes. , 2009, , 275-284.		0
441	New advances in unconventional resources: accumulation and production—introduction to the special issue. Frontiers of Earth Science, 2021, 15, 185-188.	2.1	0
442	Short-Timescale Chemo-Mechanical Effects and their Influence on the Transport Properties of Fractured Rock. , 2006, , 2051-2070.		0
443	Fractal Characteristics of Drilling Particle Size Distribution of Shale: A Laboratory Scale Investigation. Rock Mechanics and Rock Engineering, 2022, 55, 5307-5319.	5.4	Ο